1995

Crop Yield Mapping: Comparison of Yield Monitors and Mapping Techniques

Stuart J. Birrell, *University of Missouri*
Steven C. Borgelt, *University of Missouri*
Kenneth A. Sudduth, *United States Department of Agriculture*

Published 1995

2 Crop Yield Mapping: Comparison of Yield Monitors and Mapping Techniques

Stuart J. Birrell
Steven C. Borgelt

Dep. of Agricultural Engineering
University of Missouri
Columbia, Missouri

Kenneth A. Sudduth

Cropping Systems and
Water Quality Research Unit
USDA—Agricultural Research Service
Columbia, Missouri

Although the variability in soil nutrients and crop yields has been well documented since the turn of the century (Robinson & Lloyd, 1915; Fairfield Smith, 1938), the mechanization of agriculture and the trend to larger implements has led to larger areas being treated as a single unit. Recent advances, however, in machine technology and improvements in data management have made it possible to reverse this trend by implementing site specific crop management (Goering, 1993).

The implementation of spatially selective field operations is dependent on field mapping of the variations in soil and crop parameters (Stafford et al., 1991). The mapping of crop yield is especially important since the recommendation rates for many inputs are determined by the yield goal, and yield maps are necessary to assess the effects of site specific crop management. Since yield maps may be used both for the determination of management inputs and to evaluate the results of these strategies, it is important that the accuracy of the yield map be considered.

Recently, continuous grain flow monitors in conjunction with speed sensors and location systems have been used to develop crop yield maps (Searcy et al., 1989; Wagner & Schrock, 1989; Colvin, 1991, Stafford et al., 1991, Vansichen & De Baerdemaeker, 1991; Schnug et al., 1992; Auernhammer et al., 1993; Birrell et al., 1993; Pringle et al., 1993; Stott et al., 1993). When compared with the mass of grain accumulated over a certain time, the accuracies of the grain flow monitors are generally reported to be within 5 percent. All of the monitors reported on to date, however, measure the flow of grain into the grain bin. This flow must then be related to the flow of grain into the combine head, which requires modelling of the grain flow dynamics through the combine. Searcy et al., (1989) and Vansichen and De Baerdemaeker (1991) both suggested modelling the grain flow through the combine as a first order system with a time lag. Although the actual system dynamics of the combine may be of a higher order, the accuracy of the grain flow sensors probably does not warrant the use of a higher order model. Higher order models would also make the system more susceptible to noise or errors in the input data.

The development of grain yield maps requires that instantaneous grain yields be averaged or interpolated to obtain an estimate of the average yield within a certain area. The unit cell size and the mathematical methods used to generate the maps can have a significant effect on the results. Furthermore, sudden changes in the harvesting speed can cause large errors in the instantaneous yield. These errors are particularly large when the combine stops suddenly, which causes the calculated instantaneous yield to approach an infinite spike, since a finite volume of grain is divided by an area approaching zero (velocity times swath width). These spikes can have a significant effect on the calculation of yield in the local region around the point.

Objectives

1. Investigate the use of different combine grain flow models to determine instantaneous grain yield.
2. Analyze the effect of different Kriging parameters and combine models on the mapping of grain yield.
3. Investigate the effect of using evenly spaced transects instead of yield data collected continuously across the field to develop yield maps.

Equipment and Instrumentation

Two instrumented combines, a 3-row John Deere 3300 combine and a 6-row Gleaner R62 combine, were used to collect yield data within the same field. The combine yield mapping systems consisted of four components: (1) Global Positioning System (GPS) receivers to determine combine location; (2) a combine mounted grain flow sensor; (3) a sensor to measure ground speed; and (4) a data acquisition system. In addition, the John Deere combine had a weigh bin mounted in the combine grain tank that was used to measure accumulated grain from the grain sensor for calibration of the system.

Two Ashtech M-XII GPS receivers were used for position location (Harrison et al., 1992) when harvesting with either combine. The receivers were used in the post-process differential mode with the clear access (C/A) code. This mode of operation provided robust data acquisition with improved accuracy as compared to a stand-alone receiver. The receivers were set to record a position every 5 s. The fixed receiver remained over a known geo-referenced point and the rover receiver was placed in the combine, with the GPS antenna fixed on top of the combine cab. During harvest the necessary files required for post the GPS satellite signal were internally stored in the respective receivers. The receivers were able to store up to eight hours of data. The GPS files in the receivers were then downloaded into a computer for processing at the end of each day's harvest.

The John Deere 3300 3-row combine was equipped with a volumetric Claydon Yieldometer (Bae et al., 1987). This yield sensor measured the volume flow of grain from the clean grain elevator. A capacitive level sensor controlled the rotation of a six-flight paddle wheel, to maintain the level of grain above the paddle within certain thresholds. The standard yieldometer was modified by replacing the standard 2 counts/revolution sensor connected to the shaft of the paddle wheel with an angular position encoder (1024 counts/revolution). A DICKEY-john radar gun was mounted on the combine to measure ground speed and travel distance. A DMC moisture sensor was installed below a hole cut into the grain bin fill auger, with a solenoid used to control grain flow to the moisture sensor.

The Gleaner R62 combine was instrumented with an impact-based, AgLeader™ Yield Monitor 2000™. This sensor measured the force of the grain impacting against a plate situated at the top of the clean grain elevator. The force and other parameters such as elevator speed were then used to determine mass grain flow rate. A DMC moisture sensor was also installed directly into the grain bin auger, where a small section of auger flighting was removed. A magnetic pick-up on the drive train was used to measure ground speed. The AgLeader system also included a monitor which displayed instantaneous values and cumulative totals for parameters such as yield, grain moisture, grain flow, speed and distance. Although the monitor only stored the cumulative totals for each load, it could also output the following parameters to a RS-232 serial port on 1 s intervals: ground speed pulses; ground speed (mph); area count flag; elevator speed (rpm); grain flow sensor force (lb); grain flow rate (lb/sec); instantaneous yield (bu/ac); and grain moisture (% wet basis).

Both combine data acquisition systems relied on a portable computer running essentially the same software. The computer received the uncorrected GPS position and GPS time over one serial port, and the yield monitor data, either via the parallel port or a s serial port, on 1 s intervals. In the John Deere combine, the analog and digital signals from moisture sensor, volumetric yield monitor and speed sensor were input into an IOtech Daqbook™ data acquisition box and transferred to the computer through the parallel port. The Gleaner system with the impact-based yield monitor logged its output into the computer over a RS-232 serial port. Selected information such as position, total harvest area, and instantaneous yield were displayed on the computer screen. One window of the screen was dedicated to display the trajectory of the combine superimposed over the field boundaries. The program had the capability to show any selected information as text, a bar graph or a strip chart.

Procedures

The test field was located at the Missouri Management Systems Evaluation Area (MSEA) near Centralia, MO. The volumetric monitor was used to harvest a pair of transects every 100 m. The remainder of the corn (Zea mays L.) in the field was harvested using the impact-based monitor.

The radar gun and volumetric yield sensor on the John Deere combine were calibrated by flagging the beginning and end of a transect of known distance, while collecting the grain in the weigh bin situated in the combine clean grain tank. This was repeated several times and a linear least squares regression was used to calibrate the recorded counts to distance and mass respectively (Table 2-1). The magnetic pickup on the Gleaner combine was calibrated prior to harvest by travelling along a known distance at normal harvest speeds. The grain flow rate measurement was calibrated by comparing the nominal accumulated grain mass (kg/load) recorded by the impact-based monitor to the total mass of grain unloaded into the grain truck.

The GPS files stored in the receiver were post-processed to obtain a differentially corrected position coordinate for the combine every 5 s. The GPS time associated with the corrected positions was then matched to the UTC time that was logged to the computer over the RS-232 serial port during harvest. These times were used to replace the uncorrected positions with the post-processed differential positions. The positions between each differential correction were calculated using a linear interpolation based on time.

Table 2-1. Least squares linear regression for yield and distance calibration for the John Deere 3300 combine and Gleaner R62 (with impact-based monitor) combines.

	DISTANCE (meters)		YIELD (kg)	
	JD 3300	Gleaner	JD 3300	Gleaner
R Squared	0.998	-	0.997	0.993
Intercept	0	-	0	0
Std. Error of Y estimate	3.3108	-	15.00	1991.936
Regression slope coefficient	0.01000	0.02217	0.005653	2.6872
Std. Error of slope coefficient	0.00002	-	0.000023	0.035476
Degrees of Freedom	141	-	77	22

Data Analysis

For yield mapping, the measured grain flow f(t) must be related to the rate of grain flow r(t) into the combine head. The rate grain flow into the combine head can then be related to the yield since the velocity v(t), swath width (w) and position (x,y) of the combine are known. If the combine system dynamics are modelled as a simple time delay (p), then the yield y(t), can be calculated directly by dividing the measured grain flow at any instant by the area covered p seconds previously. For discrete sampling the yield can expressed as

$$y(i-p/T-s/2T) = \frac{\sum_{j=i-s/T}^{i} f(j)}{\sum_{k=i-p/T-s/T}^{i-p/T} d(k)} \cdot \frac{1000}{w} \tag{1}$$

where y(i) is the calculated yield (kg/hectare), f(i) is the measured grain flow (kg) and d(i) is the distance (m) travelled during the sampling period T. The delay time is p and s is the interval over which a running average yield is calculated.

In the continuous time domain, a first order system is expressed as

$$f(t) = r(t)(1-\exp((t-p-t_o)/\tau)) \tag{2}$$

where f(t) is the measured grain flow, r(t) is the grain flow into the combine head, t_0 is the time the combine started harvesting and τ is the time constant. The first order system can be written in the Laplace domain as

$$G(s) = \frac{F(s)}{R(s)} = \frac{e^{-pTs}}{(1 + \tau s)} = \frac{1/\tau \; e^{-pTs}}{(1/\tau + s)} \tag{3}$$

where G(s) represents the transfer function from r(t) to f(t). The Laplace function must then be written in the z domain since the data collection process is discrete. There are different methods to convert to the z transform but the step-invariant transform is probably the most appropriate, since entering the crop is approximately a step input. The step-invariant transform is calculated by adding a zero order hold transform to the Laplace transfer function and then converting to the z transform.

$$G(z) = Z \, \frac{(1-e^{-Ts})}{s} \cdot G(s) \tag{4}$$

The z transform will then be

$$G(z) = \frac{(1-e^{-T/\tau})z^{-(1+p/T)}}{1-e^{-T/\tau} z^{-1}} \tag{5}$$

The discrete difference form of the z transform is

$$r(k-p/T-1) = \frac{1}{(1-e^{-T/\tau})} \cdot (f(k) - e^{-T/\tau} f(k-1)) \tag{6}$$

where r(k) is the grain flow into the combine header (k=t/T), f(k) is the grain flow monitored, p is the time delay and τ is the time constant.

Due to the on–off method of operation of the volumetric yield monitor, the raw yield counts did not increase with every reading taken on 1 s intervals, even when there was a continuous grain flow into the monitor. The yield monitor itself acted as a sample and hold system, which exhibited a varying time constant since the interval between successive rotations was determined by the flowrate. In general, successive rotations occurred within 3 s, therefore, the original raw data was modified to obtain a single reading every 3 s by accumulating the yield counts over 3 s intervals.

Instantaneous yields were calculated from the raw impact-based monitor data and the modified volumetric monitor data using both a simple time delay model and a first order system model. These models were implemented with varying time delays and time constants for the first order system and with varying degrees of smoothing of the grain flow rate and velocity data inputs. Grain flow rate and velocity inputs were smoothed using a running average with a range of averaging times. The correlations of the calculated yield using different models were determined for each transect by comparing yields on a point-by-point basis along each transect. The John Deere combine with the volumetric yield monitor harvested six pairs of transects spaced evenly across the field. The adjacent transects harvested by the Gleaner combine with the impact-based monitor were identified.

The calculated instantaneous yields were then exported to a geostatistical package for analysis and the development of yield maps by Kriging. The accuracy of yield maps is dependent on the precision of the grain yield sensor and the process used to generate the maps. The results from the different models were used to develop maps over the field with identical cell sizes (10m). When the input data sets included all of the yield transects over the field, the Kriging parameters were set to restrict the number of nearest neighbors to a maximum of 8 or 24 neighbors. When the 6 pairs of transects were used to generate the map, a maximum of 32 neighbors was used.

Results and Discussion

While the average yield for the two monitors was similar, the calculated instantaneous yields from the impact-based monitor showed considerably less noise that those from the volumetric monitor. The difference is primarily due to the discrete operation of the volumetric yield monitor, whereas the impact-based monitor more closely approximated a continuous sampling system.

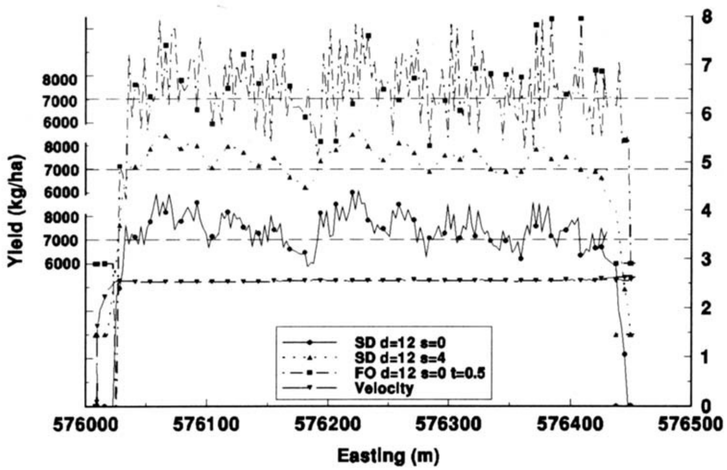

Fig. 2–1. Yield calculated from impact-based yield monitor data, using a simple time delay (SD) and a first order (FO) model with several smoothing times. (Time delay d=12s; Smoothing time s=0-4s, Time constant t=0.5s).

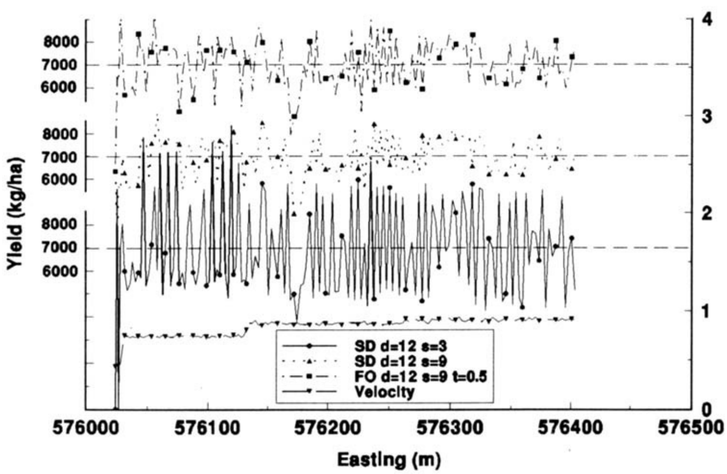

Fig. 2–2. Yield calculated from volumetric yield monitor data, using a simple time delay (SD) and a first order (FO) model with several smoothing times. (Time delay d=12s; Smoothing time s=3-9s, Time constant t=0.5s).

The instantaneous yield for the impact-based monitor was calculated using different models (Fig. 2–1). When a simple time delay model was used the calculated instantaneous yield showed little noise even with no smoothing of the raw data, and smoothing of the raw data did not significantly improve the calculated yield. When a first order model was used without smoothing, however, the calculated yield displayed a high frequency noise component due to the amplification of the higher frequencies in the raw data caused by the inversion of the first order system. When the raw data was smoothed, the calculated yield from the first order system approached that from a simple time delay model (Fig. 2–1). The smoothed first order and simple time delay model yields were very similar except when entering the crop, where the first order delay model more closely modelled the step change in yield. Since the yields calculated, however, when a large change in velocity occurred were unreliable and probably should be disregarded, there would be little advantage to modelling this step change in yield.

The instantaneous yield for the volumetric monitor was calculated using various models (Fig. 2–2). The simple time delay model showed a substantial amount of noise with no smoothing of the modified raw data. If the modified raw data was smoothed the local trends in yield could be seen (Fig. 2–2). When a first order system was used, the high frequency noise began to dominate the signal, even with smoothing of the model input data. This was caused by the discrete operation of the monitor. Theoretically, the monitor could be modelled as an additional first order system. The time constant of this model would vary with yield, however, adding another unknown parameter to the complete system model. Figures 2-3 and 2-4 show the calculated instantaneous yield for a pair of east-west transects for the impact-based monitor and volumetric monitor, respectively. As expected, the transects show similar local trends, although this was less apparent with the volumetric monitor.

The correlation coefficients between the instantaneous yields obtained using the different models were calculated for each transect. Table 2-2 shows the correlation coefficients between a single "reference" model and the other models for each monitor. The same number was used to identify a single pair of transects harvested adjacent to each other and the letters were used to separate the individual transects. The impact-based monitor showed a high correlation between simple time delay models with different smoothing intervals. When a first order system was used with no smoothing, the correlation between this model and the simple delay models was low. When the amount of smoothing was increased, the correlation between the first order system and simple time delay systems increased. The reverse was true if the time constant was increased (Table 2-2). The volumetric monitor showed similar trends, except the degree of smoothing required to increase the correlation was much greater. The first order systems showed considerable high frequency noise which was reflected in the lower correlations between the models (Table 2-2).

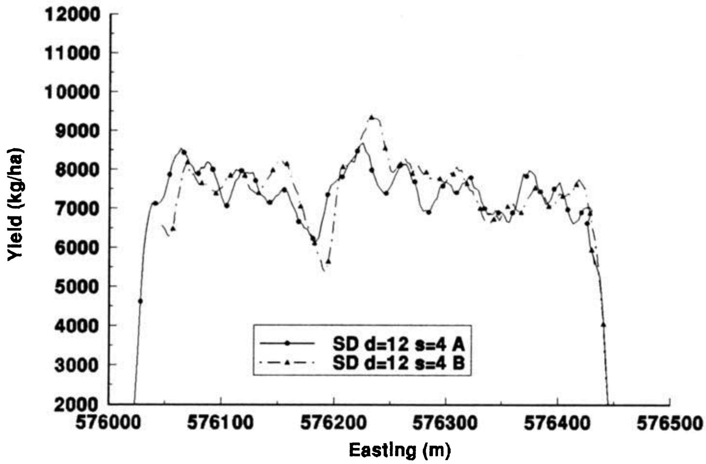

Fig. 2–3. Yield calculated from impact-based yield monitor data for a pair of side by side transects, using a simple time delay (SD) model. (Time delay, d=12s; Smoothing time s=0s)

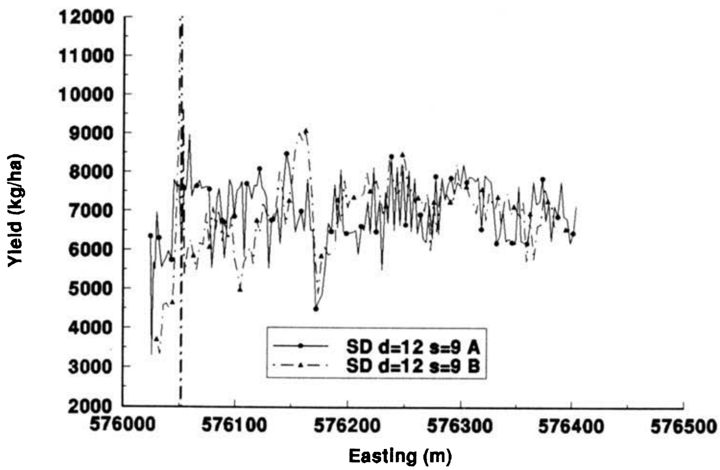

Fig. 2–4. Yield calculated from volumetric yield monitor data for a pair of side by side transects, using a simple time delay (SD) model. (Time delay, d=12s; Smoothing time s=9s)

Table 2-2. Correlations between a selected reference model and the Simple Time Delay (SD) and First Order (FO) combine models with different degrees of smoothing (Time delay(d) =12s; Time constant(t) =0.5 or 0.3s; Smoothing time(s)=0-21s).

TRANSECT	1A	1B	2A	2B	3A	3B	4A	4B	5A	5B	6A	6B	1A-6B
GLEANER COMBINE: Correlation of different models with simple time delay model with no smoothing (SD d=12s, s=0s)													
SD d=12s, s=0s	1.00	1.00	1.00	1.00	1.00	1.00	1.00	1.00	1.00	1.00	1.00	1.00	1.00
SD d=12s, s=4s	0.92	0.94	0.74	0.94	0.97	0.93	0.89	0.94	0.94	0.95	0.96	0.91	0.92
FO d=12s, s=0s, t=0.5s	0.08	0.16	-0.31	0.09	0.56	0.22	0.09	0.26	0.23	0.32	0.34	0.22	0.19
FO d=12s, s=4s, t=0.5s	0.67	0.72	0.45	0.74	0.86	0.70	0.48	0.71	0.74	0.73	0.68	0.63	0.68
FO d=12s, s=0s, t=0.3s	-0.11	-0.04	-0.41	-0.11	0.39	0.03	-0.06	0.08	0.03	0.11	0.11	0.03	0.00
FO d=12s, s=4s, t=0.3s	0.37	0.45	0.30	0.48	0.79	0.53	0.32	0.58	0.54	0.56	0.44	0.47	0.49
JOHN DEERE COMBINE: Correlation of different models with simple time delay model with 15 second smoothing (SD d=12s, s=15s)													
SD d=12s, s=3s	0.41	0.51	0.49	0.25	0.16	0.44	0.53	0.35	0.46	0.56	0.46	0.44	0.42
SD d=12s, s=15s	1.00	1.00	1.00	1.00	1.00	1.00	1.00	1.00	1.00	1.00	1.00	1.00	1.00
SD d=12s, s=21s	0.83	0.94	0.93	0.66	0.64	0.92	0.93	0.47	0.89	0.95	0.94	0.90	0.83
FO d=12s, s=3s, t=0.5s	0.30	0.44	0.44	0.05	0.15	0.28	0.41	-0.12	0.38	0.38	0.48	0.35	0.30
FO d=12s, s=15s, t=0.5s	0.65	0.86	0.82	0.39	0.37	0.84	0.85	0.15	0.82	0.86	0.86	0.72	0.68
FO d=12s, s=3s, t=0.3s	0.24	0.35	0.36	0.02	0.12	0.20	0.32	-0.15	0.30	0.29	0.42	0.28	0.23
FO d=12s, s=21s, t=0.3s	0.80	0.93	0.88	0.78	0.72	0.89	0.88	0.76	0.86	0.91	0.87	0.84	0.84

When yield semi-variograms were calculated over 300m, the best fit was obtained with a linear variogram that displayed a high nugget variance for all models. If the variograms were calculated over 100m, however, the simple time delay models and highly smoothed first order systems exhibited either an exponential or spherical semi-variogram, with low nugget variance and a definite spatial range (generally 25–30m). The first order systems with little smoothing displayed no spatial relationship. Theoretically, if a large active range is used the data should be de-trended before the calculation of the semi-variance. Since the neighborhood used during Kriging was restricted, however, and only the low lags of the semi-variogram were used, the Kriged output map essentially showed the local trend.

The complete set of raw impact-based monitor harvest data was used to generate yield maps, using different combine models and Kriging parameters (Fig. 2–5 through 2–8). A simple time delay model with no smoothing (Figs. 2–5 and 2–6) and a first order model with no smoothing were used (Fig. 2–7 and 2–8). The active range for the calculation of the semi-variance was 100m for Fig. 6 and 8 and 300m for Fig. 2–5 and 2–7. During Kriging the number of known points used for the calculation of the grid cell was restricted to 8 or 24 neighbors, for Fig. 2–6 and 2–8, and Fig. 2–5 and 2–7, respectively. The general trends were the same for all of the maps. When the number of known samples used in the Kriging process was reduced the trends did not change but the local variability increased as shown in Fig. 2–6 and 2–8. When a first order system as used (Fig. 2–7 and 2–8) the maps show a much higher yield along the edge of the field than when a simple time delay model was used (Fig. 2–5 and 2–6), due to the step response of the first order system. The calculated yields are probably higher than the actual yields, however, and the error associated with the calculation at these transition points was high.

Six pairs of transects 100m apart harvested by the Gleaner combine with the impact-based monitor were used to generate a map, using a simple time delay model with 4 s (Fig. 2–9). While much of the fine detail was lost, the general trends were very similar to the previously shown general field trends' (Fig. 2–5 through 2–8). Adjacent pairs of transects harvested by the Deere combine with the volumetric monitor, were used to generate a map, using a simple time delay model and 15 s of smoothing (Fig. 2–10). Although further detail was missing the basic trends were the same. Although there were some differences between the maps developed from transects as compared to those developed from a complete set of data, the transect maps do show the general trends and were a reasonable representation of yield trends. However the accuracy of these transect-based maps would also depend on the location of the transects relative to important changes in yield.

The correlations between the Kriged maps were compared on a cell by cell basis (Table 2–3). All of the whole-field simple time delay models exhibited a high correlation with each other. The unsmoothed first order system exhibited a low correlation when compared to the simple time delay maps, due to the high frequency component introduced. The transect maps developed from the Gleaner combine were reasonably correlated to the maps from the whole field data, but the John Deere combine transects showed a lower correlation.

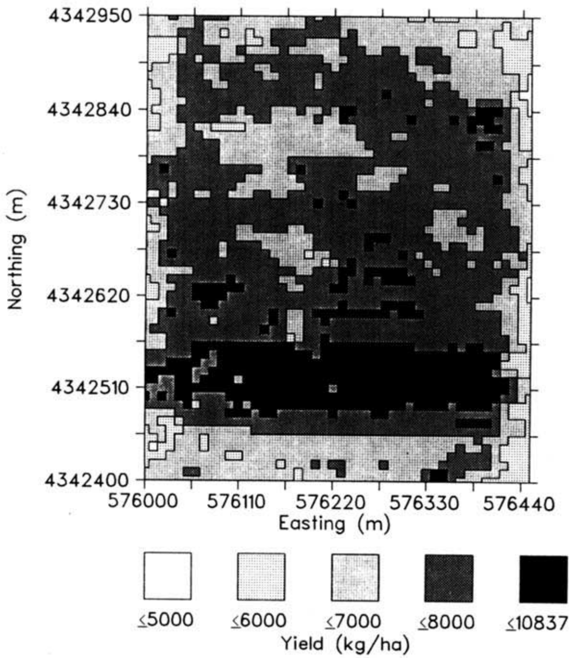

Fig. 2-5. Yield map developed from impact-based monitor data using a simple time delay model with no smoothing. Kriging semi-variogram restricted to 100m and a maximum of 8 neighbors for interpolation.

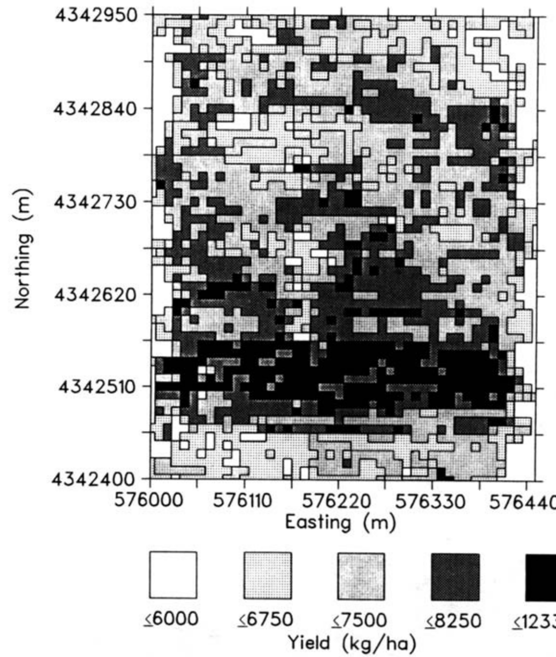

Fig. 2-6. Yield map developed from impact-based monitor data using a simple time delay model with no smoothing. Kriging semi-variogram restricted to 300m and maximum of 24 neighbors for interpolation.

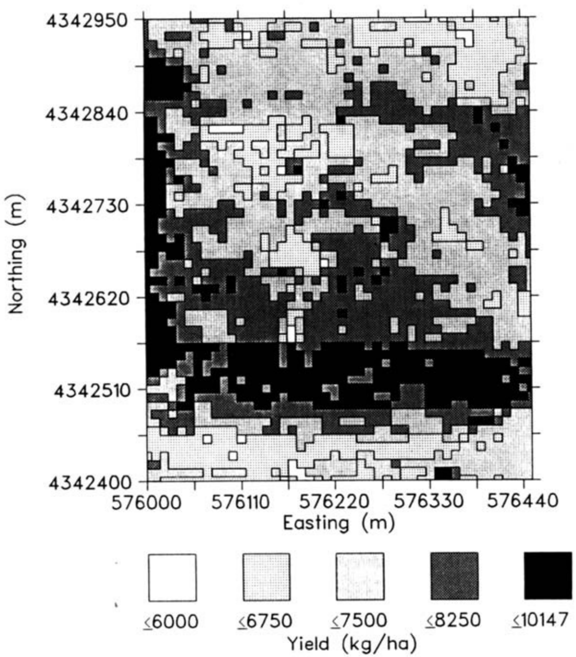

Fig. 2-7. Yield map developed from impact-based monitor data using a first order model with no smoothing. Kriging semi-variogram restricted to 300m and a maximum of 24 neighbors for interpolation.

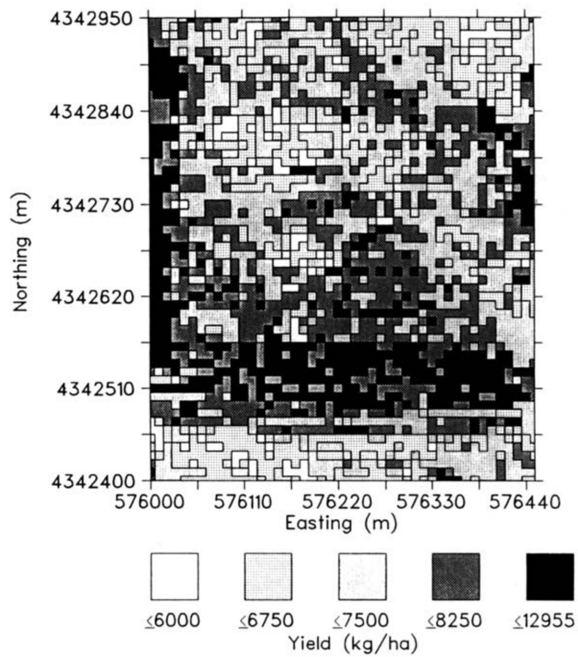

Fig. 2-8. Yield map developed from impact-based monitor data using a first order model with no smoothing. Kriging semi-variogram restricted to 100m and a maximum of 8 neighbors for interpolation.

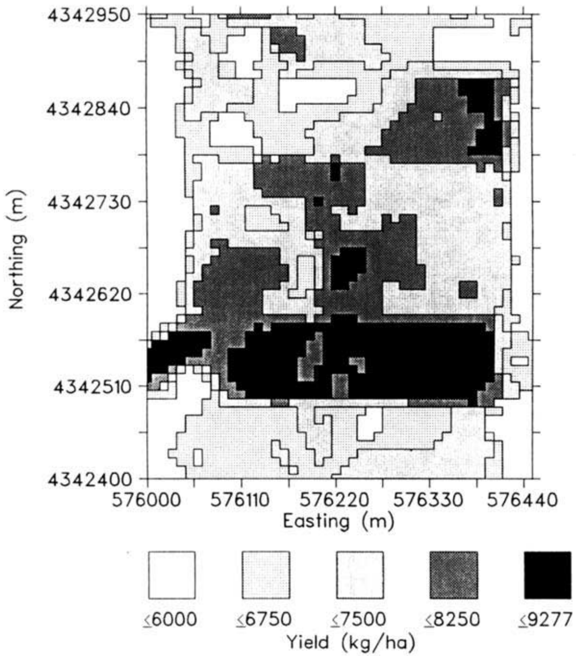

Fig. 2-9. Yield map developed using six pairs of transects of impact-based monitor data using a simple time delay model with 4 s smoothing. Kriging semi-variogram restricted to 300m and a maximum of 32 neighbors for interpolation.

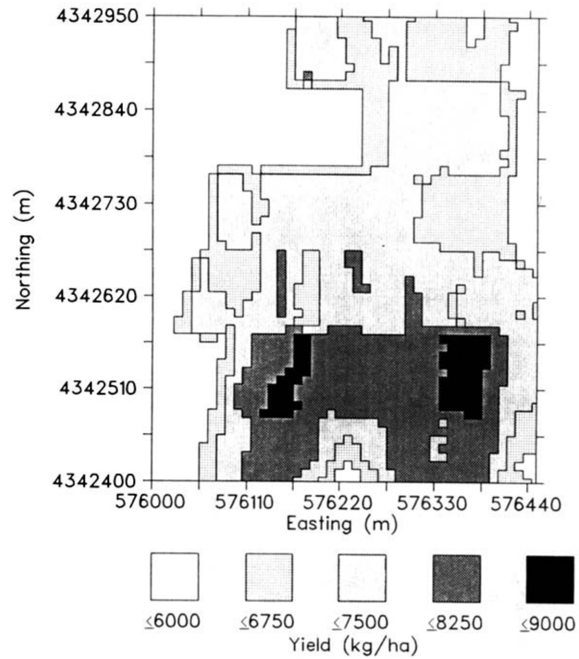

Fig. 2-10. Yield map developed using six pairs of transects of volumetric monitor data using a simple time delay model with 15 s smoothing. Kriging semi-variogram restricted to 300m and a maximum of 32 neighbors for interpolation.

Table 2–3. Correlations calculated for Kriged maps developed with different combine models and Kriging parameters. (Compared to map developed from Gleaner combine data with a simple delay model, no smoothing and 300m active Kriging range.)

Data Source	Model Type	Smoothing (s)	Time Constant (s)	Kriging Parameters		Correlation Coefficient
				Semi-variogram Active Range (m)	Number of Neighbors	
Gleaner (all data)	Simple Time Delay	0		300	24	1
Gleaner (all data)	Simple Time Delay	0		100	8	0.91
Gleaner (all data)	Simple Time Delay	4		300	24	0.9
Gleaner (all data)	Simple Time Delay	4		100	8	0.81
Gleaner (all data)	First Order System	0	0.5	300	24	0.58
Gleaner (all data)	First Order System	0	0.5	100	8	0.49
Gleaner (all data)	First Order System	4	0.3	300	24	0.68
Gleaner (all data)	First Order System	4	0.3	100	8	0.61
Gleaner (transects)	Simple Time Delay	4		300	32	0.64
JD 3300 (transects)	Simple Time Delay	15		300	32	0.41

The lower correlation for the John Deere combine transects was due to the increase in the amount of smoothing required, which removed the yield variation over short distances. In general, it appears that a simple time delay model with minimal smoothing provided the best yield maps. Maps generated from evenly spaced transects, however, showed the general yield trends and would provide useful information.

Summary

Modelling of the instantaneous yield response for two different yield monitors was investigated. Both simple time delay and first order models appeared to be reasonable models of the combine flow dynamics. The simple time delay model was less susceptible to noise but did not accurately model the step change in yield seen when entering or exiting a crop. The first order system modelled the step yield input but was highly susceptible to noise and required smoothing of the raw data. The Kriging of instantaneous yield to develop maps was fairly robust if a complete data set was used. The general trends in the data were evident even when cell values were calculated from a very localized region. Evenly spaced transects could be used to develop maps showing general yield trends although some detail is lost.

ACKNOWLEDGEMENT

We would like to thank Dr. S. W. Searcy and the Department of Agricultural Engineering, Texas A&M University, for the loan of the Claydon Yieldometer.

Mention of trade names or specific products is made only to provide information to the reader, and does not constitute an endorsement by the University of Missouri or the USDA Agricultural Research Service.

REFERENCES

Auernhammer, H., M. Demmel, K. Muhr, J. Rottmeier, and K. Wild. 1993. Yield measurements on combine harvesters. ASAE 93–1506. ASAE, St. Joseph, MI.

Bae, Y.H., S.C. Borgelt, S.W. Searcy, J.K. Schueller, and B.A. Stout. 1987. Determination of spatially variable yield maps. ASAE 87–1533. ASAE, St. Joseph, MI.

Birrell, S.J., K.A. Sudduth and S.C. Borgelt. 1993. Crop yield mapping using GPS. ASAE Paper MC93–104. ASAE, St. Joseph, MI.

Colvin, T.S., D.L. Karlen, and N. Tischer. 1991. Yield variability within fields in central Iowa. *In* Automated agriculture for the 21st Century, Proc. of the 1991 Symp. ASAE Publ. 11–91, ASAE, St. Joseph, MI.

Fairfield Smith, H. 1938. An empirical law describing the heterogeneity in the yield of agricultural crops. J. Agric. Sc. XXVIII(Jan):1–23.

Goering, C.E. 1993. Recycling a concept. Agric. Eng. 74(6):25.

Harrison, J.D., S.J. Birrell, K.A. Sudduth, and S.C. Borgelt. 1992. Global positioning system applications for site-specific farming research. ASAE 92–3615. ASAE, St. Joseph, MI.

Pringle, J.L., M.D. Schrock, R.T. Hinnen, K.D. Howard, and D.L. Oard. 1993. Spatial yield variation in grain crops. ASAE Paper 93–1505. ASAE, St. Joseph, MI.

Robinson, G.W., and W.E. Lloyd. 1915. On the probable error of sampling in soil surveys. J. Agric. Sci. 7:144–153.

Schnug, E., D. Murphy, E. Evans, S. Haneklaus, and J. Lamp. 1993. Yield mapping and application of yield maps to computer-aided local resource management. *In* Proc. of the Workshop on Research and Development Issues on Soil Specific Crop Management. 14-16 April 1992. Minneapolis, MN. ASA, Madison, WI.

Searcy, S.W., J.K. Schueller, Y.H. Bae, S.C. Borgelt, and B.A. Stout. 1989. Mapping of spatially variable yield during grain combining. Trans. ASAE 32(3):826–829.

Stafford, J.V., B. Ambler, and M.P. Smith. 1991. Sensing and mapping grain yield variations. *In* Automated Agriculture for the 21st Century, Proceedings of the 1991 Symposium. ASAE Publ. 11–91, ASAE, St. Joseph, MI.

Stott, B.L., S.C. Borgelt, and K.A. Sudduth. 1993. Yield determination using a instrumented Claas combine. ASAE 93-1507. ASAE, St. Joseph, MI.

Vansichen, R., and J. De Baerdemaeker. 1991. Continuous wheat yield measurement on a combine. *In* Automated Agriculture for the 21st Century, Proceedings of the 1991 Symposium. ASAE Publ. 11-91, ASAE, St. Joseph, MI.

Wagner, L.E., and M.D. Schrock. 1989. Yield determination using a pivoted auger flow sensor. Trans. ASAE 32(2):409-413.